Conditional deletion of CB1 receptor in parvalbumin-expressing GABAergic neurons results in hearing loss and abnormal auditory brainstem response in mice

Hao-Nan Wu[1], Tianrong Hang[1], Fang-Fang Yin[2], Xiao-Tao Guo[3], Chun-Chen Pan[3], Jia-Qiang Sun[3], Jing-Wu Sun[3], Wei Shi[4], Qing-Yin Zheng[5], Chen Lin[6], and Zheng-Quan Tang[1]

[1]Anhui University
[2]Hefei Comprehensive National Science Center
[3]The First Affiliated Hospital of USTC
[4]Beihang University
[5]Case Western Reserve University
[6]University of Science and Technology of China

January 04, 2025

Abstract

Cannabinoid receptor 1 (CB1R) is widely expressed in central auditory system and play important roles in synaptic plasticity and sensory processing. However, the function of CB1R in specific neuronal subtypes in the central auditory system is largely unclear. In the current study, we investigated whether CB1R deficiency in the parvalbumin (PV)-expressing interneurons, a major class of GABAergic interneurons, affect hearing function. We fist systematically examined the neuronal localization and distribution of CB1R in mice central auditory system using double-label immunofluorescence and confocal laser scanning microscopy, and found that CB1R showed a wide distribution in the central auditory system, especially highly expressed in the cochlear nucleus (CN), superior olivary complex (SOC) and lateral lemniscus (LL). Furthermore, we established a CB1R conditional knockout mice specifically in PV interneurons, and measured auditory function using the auditory brainstem response (ABR) test. Surprisingly, analysis of ABR indicated that conditional deletion of CB1R specifically from PV interneurons significantly elevated the physiological hearing threshold, prolongated the latency of I waves, and decreased the amplitudes of I–V waves. Collectively, these results indicate that CB1R is highly expressed in CN and SOC, as well as deleting CB1R specifically from PV interneurons resulted in partial hearing loss and abnormal brainstem response. Our finding provides an anatomical basis for further investigating CB1R's function in auditory system, and suggest that CB1R expression in inhibitory PV interneurons is essential for hearing function.

1. Introduction

The type 1 cannabinoid receptors (CB1Rs) are widely expressed throughout the central nervous system (CNS) (Domenici et al., 2006; Castillo et al., 2012; Kendall and Yudowski, 2016a; Barti et al., 2024; B et al., 2024a), particularly in areas such as the hippocampus, basal ganglia, and cerebellum. Activations of CB1Rs by endocannabinoids such as 2-arachidonoyl glycerol (2-AG) and anandamide (AEA) can modulate neurotransmitter release and impact a myriad of physiological functions, such as stress, learning, memory, cognitive and sensory processing (Marsicano et al., 2002; Stachowicz, 2023; Barti et al., 2024) (Zou & Kumar, 2018). CB1Rs are expressed in both excitatory and inhibitory neurons, and their specific functions can be different depending on the type of neuron in which they are expressed. (Kendall and Yudowski,

2016b; Busquets-Garcia et al., 2018b, 2018a; Barti et al., 2024). For instance, Busquets-Garcia et al. have found that CB1Rs are predominantly expressed on certain subpopulations of GABAergic interneurons in hippocampus and the deletion of CB1Rs in these neurons impairs incidental associative learning (Busquets-Garcia et al., 2018a, 2018b). Recently, Dudok et al. have employed advanced imaging techniques to observe endocannabinoid (eCB) signaling in the hippocampal CA1 region of mice during navigation tasks, and demonstrated that CB1Rs are selectively expressed at synapses of CCK-expressing interneurons and genetic deletion of CB1Rs in these interneurons results in altered place cell firing tuning, suggesting that CB1Rs-mediated modulation of inhibitory synapses is crucial for the proper encoding of spatial information during behavior (B et al., 2024a). These above researches highlight CB1Rs importance in modulating synaptic plasticity and neuronal activity during behavior and underscore the critical role of eCB signaling in fine-tuning neural circuits involved in spatial navigation and memory formation. While much has been uncovered regarding the specific functions of CB1Rs in distinct neuronal subtypes in the central nervous system, less attention has been paid to central auditory system specifically.

CB1Rs are highly expressed in the central auditory system across several species, including rodents, humans, and other mammals (Tzounopoulos et al., 2007; Zheng et al., 2007; Y et al., 2009; Zhao et al., 2011; X et al., 2020; S et al., 2022). For instance, the distribution of CB1Rs in the adult rat brain, including the cochlear nucleus, has been investigated using receptor binding radioautography and in situ hybridization histochemistry (Mailleux and Vanderhaeghen, 1992). In the cochlear nucleus, CB1Rs are predominantly found in regions associated with synaptic processing, particularly in the dorsal cochlear nucleus (DCN) (Mailleux and Vanderhaeghen, 1992). Further studies using immunohistochemistry have confirmed CB1Rs are present in the DCN of mice (Tzounopoulos et al., 2007; Y et al., 2009; Zhao et al., 2011). Moreover, Zheng et al. have demonstrated that CB1Rs are localised to many different cell types in the cochlear nucleus of rat (Zheng et al., 2007). More recently, Alejando et al. have found that CB1Rs are expressed in inferior colliculus (IC) and auditory cortex (AC) of hamster through RT-qPCR and immunostaining (Fuerte-Hortigón et al., 2021). Consistently, evidence has suggested that CB1Rs are expressed in AC of human and non-human primate (S et al., 2022). Liu et al. have investigated the transcriptional abundance of *Cnr1* (CB1Rs encoding gene) mRNA in the brains from adult C57BL/6J mice of two sexes using RNAscope in situ hybridization (ISH) (X et al., 2020), and CB1Rs are found in the IC and AC. Although the expression of CB1Rs in the central auditory system has been extensively studied, the spatial distribution of CB1Rs across different auditory nuclei is still not fully understood.

Accumulating evidence indicate that CB1Rs in central auditory system modulate neurotransmitter release, synaptic plasticity, and may play roles in normal physiological function (18,19). CB1Rs have been implicated in the pathology of tinnitus (Zheng et al., 2007, 2015). Moreover, a previous study has suggested that deleting the CB1Rs gene does affect basic hearing abilities of mice (Anon, n.d.). However, the exact roles of CB1Rs in the central auditory system and in different types of neurons, such as inhibitory interneurons or excitatory projection neurons, remain largely unexplored.

To address these issues, we first systematically characterized the neuronal localization and distribution of CB1Rs in several central auditory nuclei of mice, including the cochlear nucleus (CN), superior olivary complex (SOC), inferior colliculus (IC), lateral lemniscus (LL), medial geniculate body (MGB), and auditory cortex (AC), using fluorescence immunohistochemical techniques. Our findings demonstrated that CB1R proteins are highly expressed in the CN, SOC and LL. We next generated conditional knockout mice with Cnr1 specifically deleted from PV interneurons, a major type of GABAergic interneurons in the central auditory system, and explored how CB1R deficiency in these neurons affects hearing function using auditory brainstem response (ABR) tests. Interestingly, the conditional deletion of Cnr1 in PV interneurons resulted in hearing loss at 32 KHz and abnormal auditory brainstem responses. This work may have broader implications for understanding how cannabinoid signaling influences sensory processing and provide further insights into CB1Rs as a potential pharmaceutical target for treating auditory dysfunctions.

2. Materials and Methods

2.1 Animals

Two types of C57BL/6J mice, *Cnr1*$^{flox/flox}$ (non-cKO) and PV-Cre;*Cnr1*$^{flox/flox}$ (Cnr1-cKO or PV;Cnr1^{cKO}) were used for the experiments. Mice were bred and housed according to the guidelines of Institutional Animal Care and Use Committee of Anhui University (protocol numbers 2020-039). Genotyping of the transgenic mice was performed using PCR and agarose gel electrophoresis with the primers listed in Table S1 to identify homozygous and hemizygous mice. The mice were housed in a facility with controlled temperature and humidity on a 12-hour light/dark cycle (lights on at 8 a.m.), and were provided with food and water ad libitum until they reached 8–10 weeks of age. In the immunostaining analysis for CB1Rs distribution, the number of non-cKO male mice used for each auditory nucleus was as follows: CN (n=10), SOC (n=7), LL (n=5), IC (n=8), AC (n=3), and MGB (n=3) (Fig. 1, Fig. 2). For the double-staining analysis of PV and CB1Rs, both non-cKO (n=5) and Cnr1-cKO (n=5) mice were used (Fig. 3). In the western blot and RT-qPCR analyses, the number of mice used were as follows: wild-type (n=5), Cnr1-cKO (n=5), and non-cKO (n=6) (Fig. S6). For the ABR tests, non-cKO (n=5) and Cnr1-cKO (n=5) mice were used (Fig. 4).

2.2 Immunostaining

Mice were anesthetized with pentobarbital sodium (60 mg/kg body weight, intraperitoneal injection), followed by transcardial perfusion with phosphate-buffered saline (0.01 M PBS, pH 7.4), and subsequently with 4% formaldehyde (PFA) prepared at 4°C to fix the tissues. The brain was extracted and fixed in 4% PFA for an additional 12 hours, after which it was transferred to 15% sucrose (in 0.01 M PBS, pH 7.4) for one day and 30% sucrose for another two days at 4°C. Subsequently, the brain was sectioned coronally into 40 μm slices using a cryostat microtome (Leica CM 1900, Leica Biosystems, Wetzlar, Germany), and the slices were collected in PBS.

The brain sections were permeabilized in a blocking solution (5% goat serum, 0.5% Triton X-100, and 0.01% sodium azide in 0.01 M PBS) for 1 hour at room temperature (RT). The sections were then incubated overnight at 4°C with primary antibodies against CB1Rs (1:5000, sc-518035, Santa Cruz) or parvalbumin (1:500, 195002, Synaptic Systems). All antibodies were prepared in the blocking solution.

After washing the sections three times for 10 minutes each in 0.01 M PBS, they were incubated with secondary antibodies: goat anti-mouse Alexa Fluor 488 (1:250, 33206ES60, Yeasen) or goat anti-rabbit Alexa Fluor 594 (1:300, 33112ES60, Yeasen) for 2 hours at room temperature (RT). The sections were then washed several times in PBS, mounted, dried, and counterstained with 4',6-diamidino-2-phenylindole (DAPI, BMU107-CN, Abbkine) before being cover-slipped. For double-staining, the sections were incubated with the individual primary antibodies and then revealed with their respective secondary antibodies. All antibodies used are listed in Table S1.

Fluorescent signals from the sections were captured using a confocal laser scanning microscope (LSM980, Zeiss) with a Plan-Apochromat 20× objective lens (effective NA = 0.8). The signal intensity of the fluorescence was semi-quantitatively analyzed using ImageJ software (NIH). The channels were separated individually, and the region of interest (ROI) was outlined to exclude background noise. The threshold for each image was adjusted to a default value, and an appropriate algorithm was selected for analysis. Fluorescence signal from the sections were captured using a confocal laser scanning microscope (LSM980, Zeiss) with a unified numerical aperture of the lens (effective NA=0.8, Plan-Apochromat 20×). The signal intensity of fluoresce was semi-quantitatively analyzed by ImageJ software (NIH). Channels were splitted individually and the region of interest was traced out to eliminate background noise. The threshold for each image was adjusted to a default value while a proper algorithm was selected.

After setting the measurements, the results of Integrated Density (IntDen) and IntDen/Area would be provided automatically. The counting of cells was performed by unbiased stereological methods referred to (West, 1999; Zhang et al., 2017). Part of the images were merged for analysis of co-localization of CB1Rs with PV.

2.3 Western Blot analysis

The Cnr1$^{flox/flox}$ and PV-Cre;*Cnr1*$^{flox/flox}$ transgenic mice were sacrificed and used for the immunoblot after

anesthesia. Brain tissues were extracted and lysed using homogenizer in ice-cold lysis buffer (20 mM Tris, pH 7.5, 150 mM NaCl, 1% Triton X-100) supplemented with protease inhibitor AEBSF and reductant β-ME. The lysate was centrifuged twice at 15,000×g for 20 min at 4 to remove insoluble debris, and the supernatant was transferred to a sterile EP-tube for another 20 min centrifugation. The concentration of total proteins in solubilized fractions was determined by Bradford assay using spectrophotometer at 595 nm. Then the protein samples were mixed with 5xLoading buffer (Dithiothreitol contained) and denatured in Block Heater for separation by 15% SDS-PAGE (Tanon Electrophoresis System). Separated proteins were transferred onto 0.22 μm PVDF membranes individually, and the membranes were blocked in TBST (20 mM Tris-HCl, pH 7.6, 150 mM NaCl, 0.05% Tween 20) with 5% non-fat milk contained for 1 hour at RT. The primary antibodies used for target and reference proteins were anti-CB1Rs (1:5000, sc-518035, Santa Cruz) and anti-GAPDH (1:5000, AF7021, Affinity) respectively, and they were further detected with HRP-linked secondary antibodies for ECL assessment (Table S1). The blotting bands were visualized with chemiluminescence imaging system (JS-1070P, Peiqing). Band intensities were quantified through ImageJ software (NIH) to analyze the protein expression of CB1Rs relative to GAPDH in the same sample.

2.4 RT-qPCR

Brain tissues isolated from mice were homogenized in Trizol, and then mixed with chloroform for 2 min of shaking and 3 min of quiescence at Room Temperature to extract total RNA. The mixture was centrifuged at 12,000×g for 15 min at 4 to separate water-organic phases. Then the water phase was preserved with isopropyl alcohol added and mixed well before precipitation at -80 degC for 2 hrs. The new mixture was centrifuged for another 15 min at 12,000xg to precipitate RNA, and then washed by ice-cold 80% ethanol. Finally, the gelatinoid RNA precipitant was desiccated and dissolved in 0.1% DEPC ddH_2O. Concentration measurement by OneDrop spectrophotometry (OD1000+, WINS) combined with integrity detection through agarose gel electrophoresis were conducted to evaluate the quality of RNA.

Reverse-transcription and quantitative real-time PCR were subsequently performed using the cDNA Synthesis Kit (11141ES60, YEASEN) and qPCR Kit (11184ES08, YEASEN) respectively. Data from qPCR were normalized with the method of 2^{-Ct}, and the relative transcription of *Cnr1* was derived from the transcript ratio of *cnr1* to*β-actin* , the reference gene. All the regents and materials used were RNase-free, and the primers used to amplify the target genes are shown in Table S2.

2.5 Auditory brainstem response (ABR) test

Since the ABR test provides auditory information of nuclei in the central pathway to sound stimulation, a TDT (Tucker Davis Technologies) RZ6 system was used to collect evoked auditory signals of mice. The mice were anesthetized with pentobarbital sodium (60 mg/kg, IP injection) and positioned 10 cm from the free-field speaker (monaural) on a non-electric heating pad (˜37 °C) with three platinum coated electrodes placed in the scalp, within the sound-proof chamber. The impedance was adjusted below 5 Ohm before recording, and sound stimuli is produced through the speaker. For click stimulus, the mouse is presented with a wide spectrum click (0.1 ms) in a gradient descent of 10 dB SPL from 90 to 10 dB SPL. Each data point acquisition was repeated for512 times and the integral signals were averaged for display. For frequency-specific tone burst stimulus, five frequencies including 4, 8, 16, 24 and 32 kHz (0.1 ms) were presented in decreasing levels between 90˜20 dB SPL, and each new stimulus was recorded 5 dB SPL down from the previous. Each point of measurement was recorded 512 times to be averaged. ABR threshold was considered as the lowest intensity of recognizable response for the given set of variables, and all the hearing threshold, latency, waveform, and amplitude of ABR data were determined using BioSigRZ software. When finished recording, the mice had electrode removed and were carefully sent to emergence from anesthesia. The ages and ambient noise levels in the vivarium were precisely matched for all the C57BL/6J mice used in ABR test, and the experimental condition was strictly controlled at each frequency to make the data valid and reliable.

2.6 Statistical analysis

In all the experiments, mice in the age of 8-10 weeks were randomly selected as biological replicates to make

the study reliable. For western-blot, the darkness of blotting-bands was integrated using ImageJ (NIH). For immunostaining, the images collected from confocal microscopy were processed by ZEN (Zeiss) and for further cell numbering or fluorescent intensity integration in ImageJ. The waveform plots exported from BioSigRZ software in ABR test were line-smoothed by Origin9 (OriginLab). Other graphs were prepared in GraphPad Prism software (GraphPad). Normality of the data was tested using the Shapiro-Wilk normality test. Nonparametric data with multiple comparisons were analyzed by Kruskal-Wallis one-way analysis of variance (ANOVA) followed by Holm's Stepdown Bonferroni procedure for adjusted P -values. The Mann-Whitney t test was used for comparison between two groups. Data with normal distribution were analyzed by one-way ANOVA with Dunnett's post-test or Tukey's correction for multiple comparisons as described in the figure legends. The data are presented as the average mean ± standard error (SEM) for data that were normally distributed or median and interquartile range for data that were not normally distributed for continuous variables. For all comparison,P and n represent the value of significance and the number of mice, respectively. $P < 0.05$ was considered statistically significant. Data were analyzed using GraphPad Prism software. Finally, the results of some statistics were presented as graphs of boxplots (whiskers), and some were presented as histograms using GraphPad Prism. The F statistic as well as the degrees of freedom and the P value were descripted in the Results section and the corresponding figure legends.

3. Results

To gain insight into CB1Rs functions specifically in inhibitory neural circuits of the central auditory system, we selectively deleted*Cnr1* by Cre dependent deletion of loxP flanked exons, which leads to an unstable protein (Marsicano et al., 2002, 2003).$Cnr1^{flox/flox}$ mice were mated with PV-Cre mice to generate mice with CB1Rs cKO specifically from PV interneurons.$Cnr1^{flox/flox}$ mice were used as controls because they retain normal levels of CB1Rs and functionality (**Fig. S1c**). Mice with two different genotypes, $Cnr1^{flox/flox}$ (non-cKO) and PV-Cre;$Cnr1^{flox/flox}$ (Cnr1-cKO), were identified and randomly separated into several groups for different purposes.

3.1 CB1Rs are highly expressed in auditory brainstem

In the current study, we first analyzed the distribution and expression of CB1Rs in the central auditory system of mice. The distribution and expression level of CB1Rs in various regions of central auditory system were both qualitatively and quantitatively evaluated using immunostaining through fluorescence imaging, and coronal sections of auditory nuclei were subjected to immunohistochemical analysis.**To investigate the characteristics of CB1Rs expression in central auditory system of $Cnr1^{flox/flox}$ mice, CB1R-immunostaining was detected in several nuclei, including** the cochlear nucleus (CN), superior olivary complex (SOC), inferior colliculus (IC), the lateral lemniscus (LL) , medial geniculate body (MGB) and auditory cortex (AC).

The expression of CB1Rs proteins in different auditory nuclei was quantitatively analyzed using average fluorescence intensity (fluorescence intensity per unit area) (Fig. 1 and Fig. 2), and total cell counting was used to address both the density of expression and the distribution of CB1R-expressing cells contained in different nuclei (Fig. 1 and Fig. 2). For each nucleus, three to five coronal sections at different distances from the bregma were used for analysis to ensure a comprehensive analysis of each nucleus.

As expected, we found that the CB1Rs are widely distributed throughout the central auditory system (Fig. 1a), particularly abundantly enriched in CN, SOC and LL. In the CN, we observed the differential expression of CB1Rs within the subregions of the CN. The VCN showed higher CB1Rs expression when compared to the DCN. Within the VCN, the anteroventral cochlear nucleus (AVCN) has significantly higher CB1Rs expression than the posteroventral cochlear nucleus (PVCN) (Fig. 2a). In SOC, CB1Rs proteins are expressed stably with similar strength across the medial superior olive (MSO), lateral superior olive (LSO), and medial nucleus of the trapezoid body (MNTB) (Fig. 2a). We observed that CB1R proteins are also detected in the MGB at a moderate expression level relative to the CN, SOC, and LL (Fig. 1a). In contrast,

CB1Rs expression in the IC) and AC was poorly detected, with almost no visible positive immunoactivity in the AC (Fig. 1a). Intriguingly, the IC showed weak expression of CB1Rs, with sporadic fluorescence signals in the dorsal central nucleus of the inferior colliculus (DCIC) and the central nucleus of the inferior colliculus (CNIC) (Fig. 2a). Moreover, our finding that the total number of CB1R$^+$ neurons was significantly higher in the SOC and LL compared to other regions is consistent with a megascopic observation (Fig. 1b). The CN ranks second in terms of the number of CB1R$^+$ neurons among all auditory nuclei, following the SOC and LL, while the IC has fewer CB1R$^+$ neurons than SOC, LL, and CN. Much fewer CB1R$^+$ neurons were identified in the MGB and AC, with relatively lower expression levels of CB1Rs proteins in these regions (Fig. 1b).

To obtain a more quantitative and detailed understanding of CB1Rs distribution, the average fluorescence intensities of CB1Rs across distinct auditory nuclei were analyzing for quantifying CB1Rs expression patterns (Fig. 1c, 2b). Average fluorescence intensities of CB1Rs are maximumly distributed in the regions of the SOC and CN, compared to the cell number calculations (Fig. 1c). While the cell numbers in the LL were almost the same as in the SOC, the average fluorescence intensity of CB1Rs in the LL was closer to the CN than to the SOC (Fig. 1c). LSO had a greater number of CB1R$^+$ neurons compared to MNTB and MSO (medial superior olive), yet the average fluorescence intensities of CB1Rs were similar across the three nuclei (Fig. 2b, 2c). The inconsistency between cell number and fluorescence intensity observed in the subregions of CN and IC further highlights the complexity of CB1Rs expression patterns across different auditory nuclei (Fig. 2b, 2c). The discrepancy between the analysis of cell number and fluorescence intensity of CB1Rs expression can indeed be attributed to a variety of factors, including the differential enrichment of CB1Rs expression in distinct brain regions and cell types, as well as the localized distribution of CB1R$^+$ neurons within specific regions.

This initial analysis of CB1Rs distribution and expression patterns within the central auditory system provides a solid foundation for further investigation into their functional role in auditory processing.

3.2 Cnr1 conditional knockout Cnr1 conditional knockout leads to a decreased distribution of CB1R$^+$ PV-neurons

To elucidate how CB1Rs influence inhibitory circuits in central auditory system and ultimately auditory signal processing, we generated the conditional knockout mice with Cnr1 specifically deleted from PV interneuron, a major type of GABAergic interneurons in the central auditory system.

To confirm the specific deletion of CB1Rs from PV neurons, we performed double-staining for CB1Rs and PV in both the PV-Cre;Cnr1$^{flox/flox}$ and Cnr1$^{flox/flox}$ mice. This approach allows us to assess the co-localization of CB1Rs and PV, providing direct evidence for the selective loss of CB1Rs in PV-expressing neurons and confirming the specificity of the conditional knockout (**Fig. 3a**). We found that average fluorescence intensity of PV (indicated by Alexa Fluor 594, red fluorescence) is nearly unchanged in Cnr1-cKO mice when compared with non-cKO controls suggests that the conditional knockout of Cnr1 does not affect the overall expression of parvalbumin in the PV$^+$ interneurons (**Fig. 3b, Fig. S2 and Fig. S3**). PV proteins are abundantly distributed in the CN and SOC, and that CB1Rs and PV proteins co-localize to a certain proportion **(Fig. 3a, 3c**).

It is not surprising that the knockout of Cnr1 specifically in PV$^+$ neurons in the PV-Cre;Cnr1$^{flox/flox}$ mice might lead to a significant change in CB1Rs expression in the CN or SOC **(Fig. 3b and Fig. 3c**). *The number of CB1R$^+$ cells was reduced in the central auditory nuclei of the Cnr1-cKO mice compared with the non-cKO controls* **(Fig. 3b**). The ratio of CB1R$^+$ PV-neurons (represented by PV$^+$/CB1R$^+$ cells) was notably decreased in the CN and SOC in the Cnr1-cKO mice **(Fig. 3c**). This suggests that the co-localization of CB1Rs and PV proteins is reduced, which could have important implications for synaptic

signaling and inhibitory control in these regions

The combination of real-time quantitative PCR (RT-PCR) and Western blotting was used to confirm the expression change of Cnr gene and CB1Rs proteins in the specific auditory regions (CN and SOC) following Cnr1-cKO **(Fig. S1**). Given the marginal anatomical definition of the CN, the region was exacted scrupulously for both western-blot and RT-qPCR. Moreover, IC and hippocampus were also exacted for RT-qPCR**(Fig. S1**). In contrast to the non-cKO group, the protein expression level of CB1Rs in the CN from Cnr1-cKO mice was significantly decreased, indicating that the conditional knockout of Cnr1 in PV interneurons led to a reduction in $CB1R^+$ neurons in this region **(Fig. S1a**). Moreover, in CN, IC, and hippocampus, the gene transcription level of Cnr1, as measured by mRNA transcripts, was also decreased in Cnr1-cKO mice, when normalized to β-actin**(Fig. S1b**).

Overall, our results indicated that deleting CB1Rs specifically from PV interneurons dramatically decreased the distribution of $CB1R^+$ PV-neurons in both the CN and SOC. This reduction in $CB1R^+$ PV-neurons was observed at both the protein and mRNA levels. The loss of CB1Rs in PV^+neurons likely disrupts the GABAergic inhibition in the central auditory system, which may lead to altered auditory signal processing.

3.3 CB1Rs cKO in PV interneurons results in hearing loss at 32 kHz

The CB1Rs were presented in many different cell types, with their expression levels dynamically varied amongst distinct subcellular locations (Kendall and Yudowski, 2016b; Busquets-Garcia et al., 2018b; B et al., 2024b). CB1Rs are recognized to have the most abundant expression in GABAergic interneurons, particularly in regions of the central auditory system such as the CN and SOC. In contrast, glutamatergic, glycinergic, and other neuronal types exhibit relatively low-to-moderate expression levels of CB1Rs (Huang and Paul, 2019). This suggests that CB1R-mediated signaling may primarily influence inhibitory circuits, especially in GABAergic interneurons, which are critical for regulating the balance between excitation and inhibition in auditory processing. The diversity of GABAergic neurons in the CNS can be characterized by multiple factors, including their transcriptomes, morphology, and electrophysiological properties. Among these, PV interneurons stand out one of the most abundant types of GABAergic neurons in the central auditory system (Hu et al., 2014; Huang and Paul, 2019). Therefore, our results suggest that loss of CB1Rs in PV interneurons might trigger abnormal hearing in mice.

To assess the impact of CB1Rs deletion in PV interneurons on hearing function, we conducted ABR tests on both Cnr1-cKO and non-cKO mice (Fig. 4 and Fig. S4). To further assess the auditory function in Cnr1-cKO and non-cKO mice, we analyzed the waveforms, thresholds, latencies, and amplitudes of waves I-V of the ABR (Fig. 4 and Fig. S4-S7). Compared with non-cKO mice, the average hearing thresholds for both click and pure-tone stimuli at 32 Hz in Cnr1-cKO mice were significantly shifted (Fig. 4b). The increased hearing thresholds in Cnr1-cKO mice indicated that the conditional knockout of CB1Rs specifically from PV-interneurons resulted in hearing loss at high frequency.

3.4 PV-Cre;$Cnr1^{flox/flox}$ mice exhibit abnormal auditory brainstem responses

Among the tone-burst stimuli with five frequencies ranging from 4 kHz to 32 kHz, the hearing thresholds in the mice presented a 'V'-shaped curve, with the lowest thresholds observed at 16 kHz, indicating that the mice had the best hearing sensitivity in this frequency range (Fig. 4b). To further evaluate the auditory function, the ABR waveforms recorded at 90 dB SPL were superimposed for both Cnr1-cKO and non-cKO mice under click and 16 kHz stimuli (with 16 kHz serving as the representative frequency). The comparison of the waveforms between the two groups revealed notable differences, especially in terms of wave amplitude and latency (Fig. 4c). Surprisingly, there were significant differences in the ABR wave characteristics between Cnr1-cKO and non-cKO groups. These differences were observed in wave amplitude, latency, and waveform morphology (Fig. 4c-e). In response to click stimuli, the amplitude of wave II in Cnr1-cKO mice decreased dramatically when compared to non-cKO mice, while the amplitudes of waves I, III, IV, and V showed only a slight decrease in Cnr1-cKO mice (Fig. 4c, 4e). Both the latencies and amplitudes of the waveforms I-V in Cnr1-cKO mice were significantly changed when compared to non-cKO mice in response to 16 kHz pure tones (Fig. 4c-e, Fig. S5-S7). Especially the wave II and wave III, which are typically linked with the

physiological functions of the CN and the SOC, respectively, were drastically changed in both amplitudes and latencies in Cnr1-cKO mice (Fig. 4c-e, Fig. S5-S7). As expected, the changes in ABR wave II and wave III were consistent with the immunostaining results from the CN and SOC in Cnr1-cKO mice, which were demonstrated previously (Fig. 3). Except for the data collected under 32 kHz, which was too ambiguous to analyze, the amplitudes of waves I-IV derived from ABR waveforms under click stimuli or other frequencies of tone burst were decreased in Cnr1-cKO mice (Fig. S6 and Fig. S7). The longer latencies and lower amplitudes observed in the ABR waveforms reflect a decrease in transduction velocity and strength of the auditory signal.

Taken together, these findings strongly suggest that the conditional knockout of Cnr1 in PV interneurons caused auditory dysfunction in mice. Specifically, the prolonged latencies indicate slower neural transmission in the auditory pathways, while the attenuated amplitudes point to a weakened neural response. This disruption in both the timing and magnitude of auditory signals in PV-Cre;Cnr1$^{flox/flox}$ mice points to the critical role of CB1Rs signaling in maintaining normal auditory processing, particularly in PV interneurons within the central auditory system.

4. Discussion

In the current study, we assessed region-specific distribution of the CB1Rs across the central auditory system of mice using fluorescence immunohistochemical techniques. Our results revealed that CB1Rs are highly expressed in the CN, SOC and LL. Furthermore, the conditional knockout of CB1Rs specifically from PV interneurons resulted in hearing loss and abnormal auditory brainstem response to a certain extent. Our findings support a functional role for CB1Rs in regulating inhibitory circuitry function in the central auditory system, ultimately impacting auditory processing.

4.1 The wide distribution of CB1Rs across the central auditory system

The ECS and its components have been the subject of extensive research, particularly for their roles in synaptic plasticity and neurodevelopment (Tzounopoulos et al., 2007; Clarke et al., 2021). While much has been studied about the ECS and its components, particularly CB1Rs, in various regions of the CNS, much less attention has been given to how CB1Rs are distributed and function in the central auditory system. Cnr1 transcripts that encode CB1Rs have been detected in various brain regions using RNA scope or in situ hybridization, however, the actual expression characteristics of CB1Rs proteins themselves-especially in the central auditory system-remain an underexplored area (Erben and Buonanno, 2019; Tao et al., 2020).

In the current study, we systematically evaluated the differentiated expression patterns of CB1Rs in the central auditory system using immunostaining. Immunostaining is an excellent way to complement in situ hybridization of mRNA transcripts, and allows for direct visualization of CB1Rs proteins in specific neuronal populations and subcellular compartments, providing valuable insights into how CB1Rs are distributed across various auditory nuclei. Our findings demonstrated that the expression of CB1Rs in the CN, SOC, IC, LL, MGB, and AC of mice are in line with previous studies, further supporting the idea that CB1Rs are widely distributed across regions of the central auditory system (Zheng et al., 2007; Zhao et al., 2011; Ji et al., 2017). Specifically, the observation that CB1Rs are particularly abundantly enriched in the CN, SOC suggest that CB1Rs play a role in modulating early auditory processing.

We also found that CB1Rs are highly expressed in PV interneurons across several auditory nuclei. The functions of CB1Rs are not solely determined by their expression levels in specific neuronal subpopulations but are also closely related to the downstream efficacy of their G protein-dependent signaling and cell-type specific signaling dynamics. For instance, in the hippocampus, where GABAergic neurons express much higher levels of CB1Rs than glutamatergic neurons, the fact that the G protein-dependent signaling of CB1Rs is less effective in GABAergic neurons suggests that CB1Rs function can be modulated by contextual factors beyond mere receptor density (Steindel et al., 2013). Likewise, the capacity of CB1Rs to modulate neurotransmission and synaptic plasticity is indeed influenced not only by their expression levels in specific cell types but also by the distinct functional properties of these cells (Huang and Paul, 2019).

4.2 Functional implications of CB1R in PV-interneurons

Although CB1Rs are present in many different cell types in the brain, the specific function of CB1Rs is largely determined by the cell type and subcellular compartment in which they are expressed. Indeed, our findings highlight an important role of cell type specific CB1Rs in hearing. In the current study, our results demonstrated that the conditional deletion of the Cnr1 gene from PV interneurons resulted in a decrease in both the number of cells expressing CB1Rs and the protein expression levels of CB1Rs, and also lead to hearing loss at 32 kHz and auditory dysfunction, as revealed by the ABR test. The transgenic mice with CB1Rs deficiency in PV-interneurons exhibited the prolongation of waves I latencies, suggesting that auditory nerve-brainstem conduction velocity is decreased. Furthermore, a decrease in the amplitudes of waves I-V observed in the transgenic mice with CB1Rs deficiency suggesting an abnormal auditory brainstem function.

The SOC plays a critical role in azimuthal sound localization, particularly in processing interaural level differences (ILD) and interaural time differences (ITD), which are essential for determining the direction of sound sources in space (Tzounopoulos and Kraus, 2009). In Cnr1-cKO mice, the significant decrease in CB1R-positive neurons and CB1Rs expression within the SOC, accompanied by drastic changes in wave II and wave III of the ABR, suggests that the CB1Rs signaling in SOC plays a crucial role in the normal functioning of auditory pathways. Therefore, the sculpting of CB1Rs expression patterns across the central auditory system would provide crucial insights into the role of CB1Rs as a neuromodulator in auditory function. The differential expression of CB1Rs in various auditory regions, especially in inhibitory interneurons like PV-positive GABAergic neurons, highlights the significant role these receptors play in regulating auditory processing, synaptic plasticity, and sound localization. Although the expression of CB1Rs in the MGB and AC was relatively low in comparison to regions like the CN, SOC and LL, the roles of CB1Rs in these auditory nuclei still warrant further exploration.

Beyond the physiological function of CB1Rs, our findings may provide insight into the biological mechanisms of the auditory dysfunction such as tinnitus (Y et al., 2015; Hwang and Chan, 2016; Pf and Y, 2016; Ji et al., 2017; Zugaib and Leão, 2018; Y and Pf, 2019). A study by Jason et al. (2011) highlighted a significant link between decreased GABAergic inhibition and hyperactivity in the DCN, which is proposed as a mechanism underlying tinnitus following noise exposure (Middleton et al., 2011). Recent studies have increasingly pointed to dysfunctional GABAergic inhibition, particularly involving PV interneurons, as a key factor in the generation or perception of tinnitus (36,48). Specifically, the changes in CB1Rs expression and the number of CB1R-positive neurons in the CN in salicylate-induced tinnitus models provide a compelling link between CB1Rs dysfunction and tinnitus (Zheng et al., 2007). The use of cannabinoid compounds, particularly tetrahydrocannabinol (THC) and cannabidiol (CBD), for the treatment of tinnitus has indeed garnered growing attention in clinical research (46,47). Therefore, the identification of CB1Rs distribution patterns across the central auditory system, coupled with an understanding of their physiological roles in GABAergic inhibitory interneurons, is crucial for unraveling the mechanisms behind auditory dysfunctions like hearing loss and tinnitus.

In summary, our findings highlight the critical role of CB1Rs in regulating PV^+ GABAergic interneuron circuits within the central auditory system. The selective deletion of CB1Rs in these cells disrupts inhibitory function, leading to hearing loss at 32 kHz and abnormal auditory brainstem responses. These results underscore the importance of CB1Rs signaling in maintaining proper auditory processing and suggest that CB1Rs dysfunction in GABAergic interneurons could contribute to auditory pathologies such as tinnitus and hearing deficits. Our study provides valuable insights into how endocannabinoid signaling, particularly through CB1Rs, influences auditory processing at the level of specific cell populations within the auditory system.

Declaration of Competing Interest

The authors declare that the research was conducted in the absence of any commercial or financial relationships that could be construed as a potential conflict of interest.

Acknowledgments

We thank Dr. Xiang-Jie Song, and Dr. Dan-Lei Bi for their technical assistance with microscopic imaging. We also extend our gratitude to Wen-Jun An and Yan-lin Wu for their support in performing the ABR tests.

Fundings

This work was supported by the Natural Science Foundation of China (Grants 32271059 and 82071061 to Zheng-Quan Tang; Grant 82271180 to Jing-Wu Sun; grant Z200024 to W.S.; Grants 81970886, 81570915 to Lin Chen), Natural Science Foundation of the Higher Education Institutions of Anhui Province (2024AH050085 to Tianrong Hang) and Anhui Provincial Natural Science Foundation for Youth (grant No. 2008085QC161 to Tian-Rong Hang).

Author Contributions

Zheng-Quan Tang, Tian-Rong Hang, Xiao-Tao Guo, Chun-Chen Pan, Jia-Qiang Sun, Jing-Wu Sun, Wei Shi, Qing-Yin Zheng and Lin Chen provided the scientific direction and the overall experimental design for the studies. Hao-Nan Wu, Tian-Rong Hang, and Fang-Fang Yin performed the molecular experiments, ABR tests and statistical analysis. Hao-Nan Wu, Tian-Rong Hang, Xiao-Tao Guo, Chun-Chen Pan, Jia-Qiang Sun, Jing-Wu Sun, Wei Shi, Qing-Yin Zheng, Lin Chen and Zheng-Quan Tang wrote the manuscript.

References

Anon (n.d.) Audiograms, gap detection thresholds, and frequency difference limens in cannabinoid receptor 1 knockout mice - PubMed. Available at: https://pubmed.ncbi.nlm.nih.gov/26427583/ [Accessed December 16, 2024].B D, Lz F, Js F, S M, J H, Dk K, C W, C R, Y L, K D, I S (2024a) Retrograde endocannabinoid signaling at inhibitory synapses in vivo. Science (New York, NY) 383 Available at: https://pubmed.ncbi.nlm.nih.gov/38422134/ [Accessed October 11, 2024].B G, K X, H M, K R, H X, Nd H, Y Z, J K, Y L, Y X, Y Z, Y Z, X Z, Z F, Jf C, H H, W W, S W (2024b) CB1R dysfunction of inhibitory synapses in the ACC drives chronic social isolation stress-induced social impairments in male mice. Neuron 112 Available at: https://pubmed.ncbi.nlm.nih.gov/37992714/ [Accessed October 11, 2024].Barti B, Dudok B, Kenesei K, Zöldi M, Miczán V, Balla GY, Zala D, Tasso M, Sagheddu C, Kisfali M, Tóth B, Ledri M, Vizi ES, Melis M, Barna L, Lenkei Z, Soltész I, Katona I (2024) Presynaptic nanoscale components of retrograde synaptic signaling. Sci Adv 10:eado0077.Busquets-Garcia A, Bains J, Marsicano G (2018a) CB1 Receptor Signaling in the Brain: Extracting Specificity from Ubiquity. Neuropsychopharmacology 43:4–20.Busquets-Garcia A, Oliveira da Cruz JF, Terral G, Pagano Zottola AC, Soria-Gómez E, Contini A, Martin H, Redon B, Varilh M, Ioannidou C, Drago F, Massa F, Fioramonti X, Trifilieff P, Ferreira G, Marsicano G (2018b) Hippocampal CB1 Receptors Control Incidental Associations. Neuron 99:1247-1259.e7.Castillo PE, Younts TJ, Chávez AE, Hashimotodani Y (2012) Endocannabinoid signaling and synaptic function. Neuron 76:70–81.Clarke TL, Johnson RL, Simone JJ, Carlone RL (2021) The Endocannabinoid System and Invertebrate Neurodevelopment and Regeneration. Int J Mol Sci 22:2103.Domenici MR, Azad SC, Marsicano G, Schierloh A, Wotjak CT, Dodt H-U, Zieglgänsberger W, Lutz B, Rammes G (2006) Cannabinoid receptor type 1 located on presynaptic terminals of principal neurons in the forebrain controls glutamatergic synaptic transmission. J Neurosci 26:5794–5799.Erben L, Buonanno A (2019) Detection and Quantification of Multiple RNA Sequences Using Emerging Ultrasensitive Fluorescent In Situ Hybridization Techniques. Curr Protoc Neurosci 87:e63.Fuerte-Hortigón A, Gonçalves J, Zeballos L, Masa R, Gómez-Nieto R, López DE (2021) Distribution of the Cannabinoid Receptor Type 1 in the Brain of the Genetically Audiogenic Seizure-Prone Hamster GASH/Sal. Front Behav Neurosci 15:613798.Hu H, Gan J, Jonas P (2014) Interneurons. Fast-spiking, parvalbumin$^+$ GABAergic interneurons: from cellular design to microcircuit function. Science 345:1255263.Huang ZJ, Paul A (2019) The diversity of GABAergic neurons and neural communication elements. Nat Rev Neurosci 20:563–572.Hwang J-H, Chan Y-C (2016) Expression of Dopamine Receptor 1A and Cannabinoid Receptor 1 Genes in the Cochlea and Brain after Salicylate-Induced Tinnitus. ORL J Otorhinolaryngol Relat Spec 78:268–275.Ji B, B C, S H, Sph A, W O, Ar P, Mn W (2017) Effects of the cannabinoid CB1 agonist ACEA on salicylate ototoxicity, hyperacusis and tinnitus in guinea pigs. Hearing research 356 Available at: https://pubmed.ncbi.nlm.nih.gov/29108871/ [Accessed October 11, 2024].Kendall DA, Yudowski GA (2016a) Cannabinoid Receptors in the Central Nervous System: Their

Signaling and Roles in Disease. Front Cell Neurosci 10:294.Kendall DA, Yudowski GA (2016b) Cannabinoid Receptors in the Central Nervous System: Their Signaling and Roles in Disease. Front Cell Neurosci 10:294.Mailleux P, Vanderhaeghen JJ (1992) Distribution of neuronal cannabinoid receptor in the adult rat brain: a comparative receptor binding radioautography and in situ hybridization histochemistry. Neuroscience 48:655–668.Marsicano G, Goodenough S, Monory K, Hermann H, Eder M, Cannich A, Azad SC, Cascio MG, Gutiérrez SO, van der Stelt M, López-Rodriguez ML, Casanova E, Schütz G, Zieglgänsberger W, Di Marzo V, Behl C, Lutz B (2003) CB1 cannabinoid receptors and on-demand defense against excitotoxicity. Science 302:84–88.Marsicano G, Wotjak CT, Azad SC, Bisogno T, Rammes G, Cascio MG, Hermann H, Tang J, Hofmann C, Zieglgänsberger W, Di Marzo V, Lutz B (2002) The endogenous cannabinoid system controls extinction of aversive memories. Nature 418:530–534.Middleton JW, Kiritani T, Pedersen C, Turner JG, Shepherd GMG, Tzounopoulos T (2011) Mice with behavioral evidence of tinnitus exhibit dorsal cochlear nucleus hyperactivity because of decreased GABAergic inhibition. Proc Natl Acad Sci U S A 108:7601–7606.Pf S, Y Z (2016) Cannabinoids, cannabinoid receptors and tinnitus. Hearing research 332 Available at: https://pubmed.ncbi.nlm.nih.gov/26433054/ [Accessed October 11, 2024].S C, T R, Kn F, Da L, Ra S (2022) Cell type specific cannabinoid CB1 receptor distribution across the human and non-human primate cortex. Scientific reports 12 Available at: https://pubmed.ncbi.nlm.nih.gov/35688916/ [Accessed October 11, 2024].Stachowicz K (2023) Deciphering the mechanisms of reciprocal regulation or interdependence at the cannabinoid CB1 receptors and cyclooxygenase-2 level: Effects on mood, cognitive implications, and synaptic signaling. Neurosci Biobehav Rev 155:105439.Steindel F, Lerner R, Häring M, Ruehle S, Marsicano G, Lutz B, Monory K (2013) Neuron-type specific cannabinoid-mediated G protein signalling in mouse hippocampus. J Neurochem 124:795–807.Tao R, Li C, Jaffe AE, Shin JH, Deep-Soboslay A, Yamin R, Weinberger DR, Hyde TM, Kleinman JE (2020) Cannabinoid receptor CNR1 expression and DNA methylation in human prefrontal cortex, hippocampus and caudate in brain development and schizophrenia. Transl Psychiatry 10:158.Tzounopoulos T, Kraus N (2009) Learning to encode timing: mechanisms of plasticity in the auditory brainstem. Neuron 62:463–469.Tzounopoulos T, Rubio ME, Keen JE, Trussell LO (2007) Coactivation of pre- and postsynaptic signaling mechanisms determines cell-specific spike-timing-dependent plasticity. Neuron 54:291–301.West MJ (1999) Stereological methods for estimating the total number of neurons and synapses: issues of precision and bias. Trends Neurosci 22:51–61.X L, X L, G Z, F W, L W (2020) Sexual dimorphic distribution of cannabinoid 1 receptor mRNA in adult C57BL/6J mice. The Journal of comparative neurology 528 Available at: https://pubmed.ncbi.nlm.nih.gov/31997354/ [Accessed October 11, 2024].Y Z, Me R, T T (2009) Distinct functional and anatomical architecture of the endocannabinoid system in the auditory brainstem. Journal of neurophysiology 101 Available at: https://pubmed.ncbi.nlm.nih.gov/19279154/ [Accessed October 11, 2024].Y Z, P R, Pf S (2015) Cannabinoid CB1 Receptor Agonists Do Not Decrease, but may Increase Acoustic Trauma-Induced Tinnitus in Rats. Frontiers in neurology 6 Available at: https://pubmed.ncbi.nlm.nih.gov/25852639/ [Accessed October 11, 2024].Y Z, Pf S (2019) Cannabinoid drugs: will they relieve or exacerbate tinnitus? Current opinion in neurology 32 Available at: https://pubmed.ncbi.nlm.nih.gov/30507635/ [Accessed October 11, 2024].Zhang C, Yan C, Ren M, Li A, Quan T, Gong H, Yuan J (2017) A platform for stereological quantitative analysis of the brain-wide distribution of type-specific neurons. Sci Rep 7:14334.Zhao Y, Rubio M, Tzounopoulos T (2011) Mechanisms underlying input-specific expression of endocannabinoid-mediated synaptic plasticity in the dorsal cochlear nucleus. Hear Res 279:67–73.Zheng Y, Baek J-H, Smith PF, Darlington CL (2007) Cannabinoid receptor down-regulation in the ventral cochlear nucleus in a salicylate model of tinnitus. Hear Res 228:105–111.Zheng Y, Reid P, Smith PF (2015) Cannabinoid CB1 Receptor Agonists Do Not Decrease, but may Increase Acoustic Trauma-Induced Tinnitus in Rats. Front Neurol 6:60.Zugaib J, Leão RM (2018) Enhancement of Endocannabinoid-dependent Depolarization-induced Suppression of Excitation in Glycinergic Neurons by Prolonged Exposure to High Doses of Salicylate. Neuroscience 376:72–79.**Figure LegendsFigure 1. Distribution analysis of CB1Rs across various auditory nuclei. (a) Immunostaining of CB1Rs in different auditory nuclei from Cnr1$^{flox/flox}$ mice. The expression of CB1R proteins in different auditory nuclei was demonstrated by fluorescence signals. CN,** cochlear nucleus**; SOC,** superior olivary complex; LL, lateral lemniscus; IC, inferior colliculus; MGB, medial geniculate body; AC, auditory cortex. CN (n=10), SOC (n=7), LL (n=5), IC (n=8), AC (n=3), and MGB (n=3). The scale-bar

for all the micrographs is 100 μm.**(b)(c) The number of CB1R-expressing neurons and the average fluorescence intensities of CB1R proteins were quantified across different auditory nuclei. The number of CB1R-expressing neurons in distinct nuclei was manually counted using the unbiased stereological method, and the average fluorescence intensity (IntDen/Area) was analyzed for each nucleus.**

Figure 2. Expression patterns of CB1Rs in subregions of central auditory nuclei. (a) Immunostaining of CB1Rs in subregions of auditory nuclei from Cnr1$^{flox/flox}$ mice. The auditory nuclei of the CN, SOC, and IC, along with their anatomical subregions, are shown in detail. DCN, dorsal cochlear nucleus; AVCN, anterior ventral cochlear nucleus; PVCN, posterior ventral cochlear nucleus; MSO, medial superior olive; LSO, lateral superior olive**;** MNTB, medial nucleus of the tapezoid body; ECIC, external cortex inferior colliculus; DCIC, dorsal cortex inferior colliculus; CNIC, central nucleus inferior colliculus. Numbers of mice used for analysis were: CN (n=10), SOC (n=7), LL (n=5), IC (n=8), AC (n=3), and MGB (n=3). **(b) Number of CB1Rs expressing neurons. The number of CB1R-expressing neurons in subregions was manually counted using the unbiased stereological method (For CN, F (2, 28) = 59.40; DCN vs. PVCN, P=0.0018; DCN vs. AVCN,P<0.0001; PVCN vs. AVCN, P<0.0001. For SOC, F (2, 36) = 80.65; MNTB vs. LSO, P= 0.0101; MNTB vs. MSO, P<0.0001; LSO vs. MSO, P<0.0001. For IC, F (2, 24) = 180.9; ECIC vs. CIC, P<0.0001; ECIC vs. DCIC, P<0.0001; CIC vs. DCIC,P<0.0001). (c) Average fluorescence intensity of CB1R proteins. The average fluorescence signal intensity was analyzed for each subregion of the CN, SOC, and IC. (For CN, F (2, 27) = 26.53; DCN vs. PVCN, P=0.0146; DCN vs. AVCN, P=0.0007; PVCN vs. AVCN,P<0.0001.For SOC, F (2, 18) = 2.559; MNTB vs. LSO,P= 0.1049; MNTB vs. MSO, P=0.2317; LSO vs. MSO,P<0.8893, For IC, F (2, 21) = 3.7; ECIC vs. CIC,P=16.94; ECIC vs. DCIC, P=15.76; CIC vs. DCIC,P=1.185).The data are presented as means ± standard error of the mean (SEM). *p < 0.05, **p < 0.01, ****p < 0.0001.**

Figure 3. CB1R knockout decreases the distribution of CB1R$^+$ PV-neurons. (a) Double staining of PV and CB1Rs. The immunoreactivity for PV is shown in red, while CB1Rs are shown in green. Co-localization of the two markers in the CN and SOC regions is depicted in yellow (merged). The number of mice used for the double-staining analysis was: non-cKO**: non-cKO (n=5) and Cnr1-cKO (n=5). (b) Comparison of PV and CB1Rs expression. The number of CB1R$^+$ neurons in the CN and SOC was manually counted for each subregion, and the results were compared between PV-Cre;Cnr1$^{flox/flox}$ and control groups.**

Similarly, the analysis of PV$^+$ neurons was performed. The average fluorescence intensity of PV was also quantified for each subregion of the CN and SOC. The data are presented as means ± standard error of the mean (SEM) (For the average fluorescence intensity of PV, the interaction between non-cKO and Cnr1-cKO was significant: F (5, 62) = 8.066; main effect of Cnr1-cKO: F (1, 62) = 18.45). For total numbers of CB1R$^+$ neurons, the interaction between non-cKO and Cnr1-cKO: F (5, 61) = 50.83; main effect of Cnr1-cKO: F (1, 61) = 569.1. DCN, P<0.0001; PVCN, P=0.0155; AVCN,P<0.0001; MNTB, P<0.0001; MSO,P<0.0001; LSO, P<0.0001). *p< 0.05, **p < 0.01, ****p < 0.0001. (c) Co-localization analysis of PV and CB1Rs in the CN and SOC. The ratios of PV$^+$ neurons expressing CB1Rs were calculated and compared with those lacking CB1Rs.

Figure 4. PV-Cre;Cnr1flox/flox mice exhibit hearing loss and abnormal auditory brainstem responses. (a) ABR Waveform Analysis. The ABR waveforms were recorded under click and 16 kHz tone burst stimuli. The black line represents the non-cKO mice (Cnr1$^{flox/flox}$), while the red line represents the Cnr1-cKO mice (PV-Cre;Cnr1$^{flox/flox}$). The numbers of mice used for the analysis were: non-cKO (n=5) and Cnr1-cKO (n=5). (b) Hearing Thresholds Obtained from ABR Waveforms. The hearing thresholds for each mouse were recorded under click and pure-tone stimuli across five frequencies (4-32 kHz) and analyzed from their ABR waveforms.

Statistical analysis showed significant differences between the non-cKO and Cnr1-cKO groups (The interaction between non-cKO and Cnr1-cKO: F (4, 30) = 3.586; main effect of Cnr1-cKO: F (1, 30) = 26.97. 4 kHz, P=0.1450; 8 kHz, P=0.1450; 16 kHz, P=0.9995; 24 kHz, P=0.5990; 32 kHz, P<0.0001). (c) Superimposition of ABR Waveforms. The ABR waveforms at 90 dB SPL, recorded under click and 16 kHz tone burst stimuli, were superimposed to highlight the differences in amplitude and latency for waves I-V between the non-cKO (black line) and Cnr1-cKO (red line) transgenic mice. This comparison reveals discrepancies in the wave characteristics between the two groups. (d) The latency and (e) amplitude from ABR waveforms. Latency and Amplitude from ABR Waveforms. The latencies and amplitudes for each ABR wave (I-V) were calculated from the ABR data collected at 90 dB SPL under a 16 kHz tone burst. Additionally, the amplitudes obtained from ABR data collected at 90 dB SPL under click stimuli are also presented. These measurements reveal significant differences in the auditory brainstem responses between non-cKO and Cnr1-cKO mice. The data are presented as means ± SEM (For the latency, the interaction between non-cKO and Cnr1-cKO: F (4, 30) = 2.406; main effect of Cnr1-cKO: F (1, 30)=15.45. I Wave, P=0.9985; II Wave, P=0.9500; III Wave,P=0.0103; IV Wave, P=0.0274; V Wave, P=0.2366. For the amplitude under 16 kHz, the interaction between non-cKO and Cnr1-cKO: F (4, 26)=2.359; main effect of Cnr1-cKO: F (1, 26)=16.50. I Wave, P=0.5682; II Wave, P=0.0004; III Wave,P=0.7907; IV Wave, P=0.8171; V Wave, P=0.8606. For the amplitude under click, the interaction between non-cKO and Cnr1-cKO: F (4, 28) = 28.68; main effect of Cnr1-cKO: F (1, 28)=13.46. I Wave,P=0.0023; II Wave, P<0.0001; III Wave,P<0.0001; IV Wave, P=0.0519; V Wave,P<0.0001). *$p < 0.05$, **$p < 0.01$, ****$p < 0.0001$.

Figures

Figure. 1

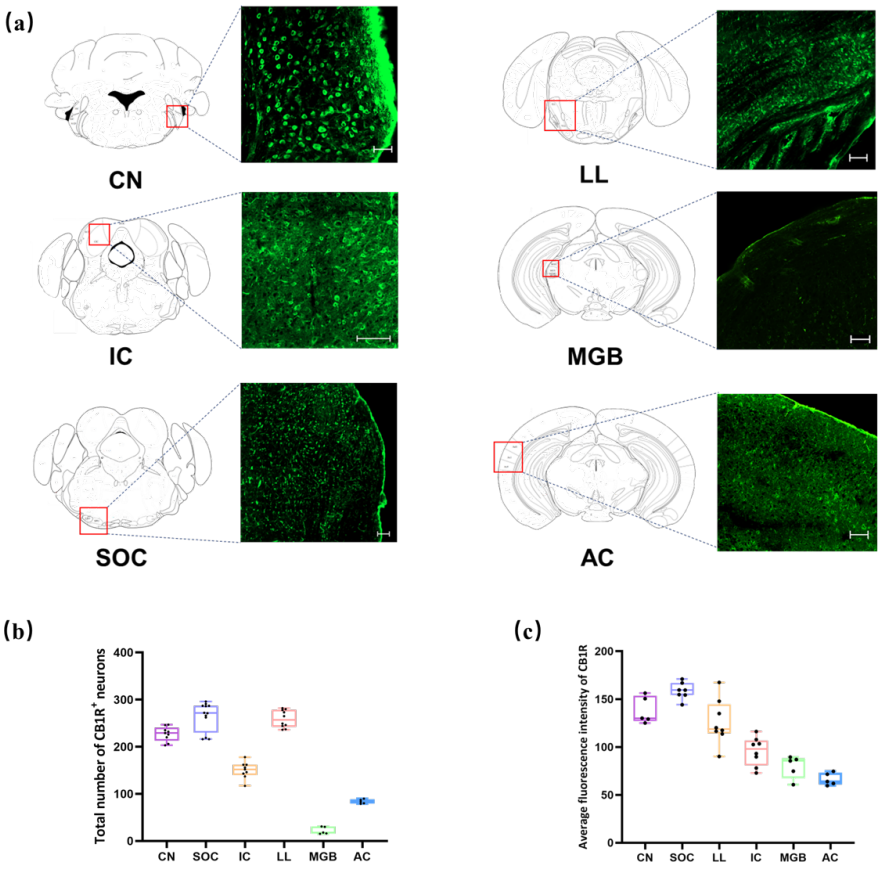

Figure. 2

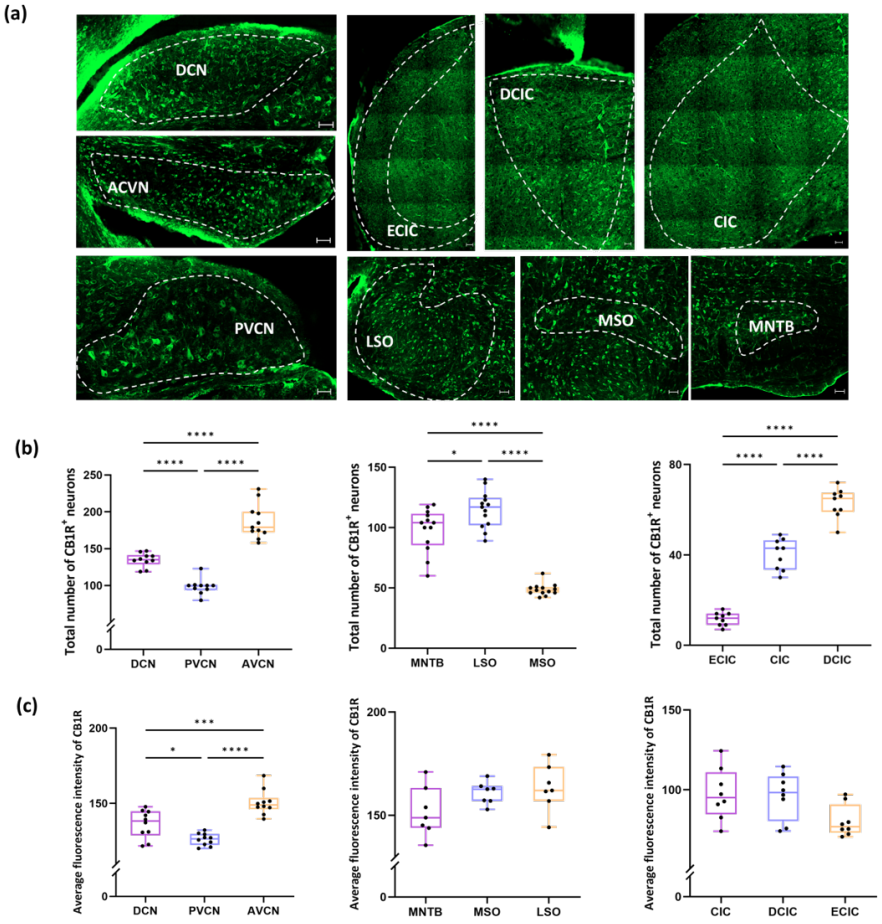

Figure. 3

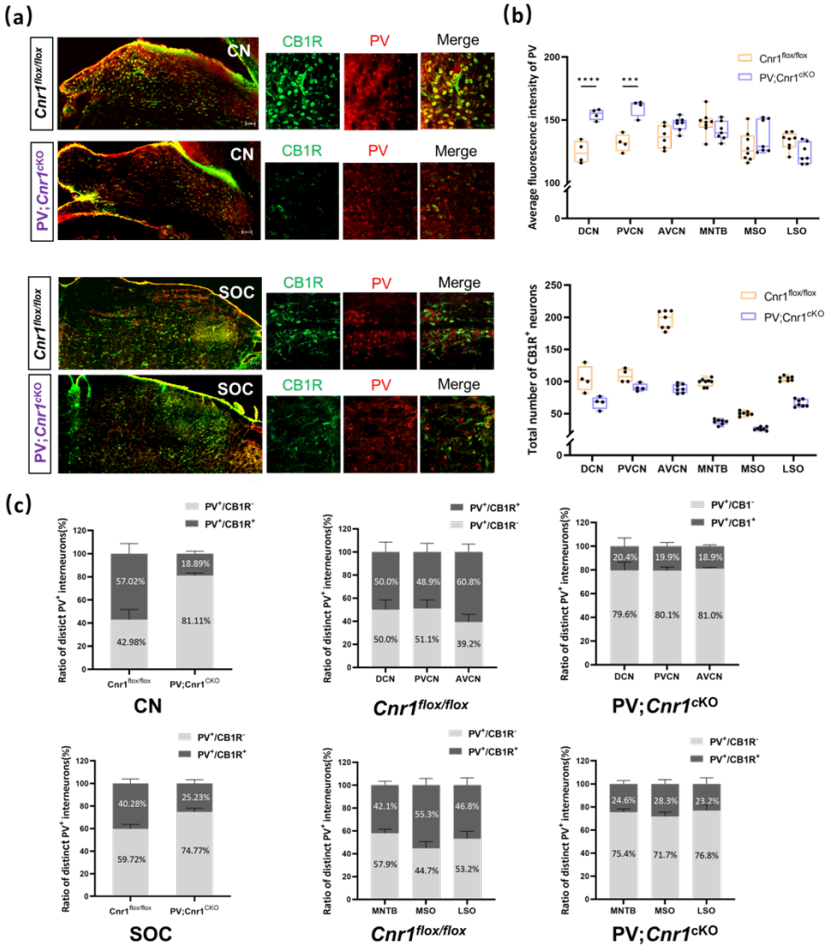

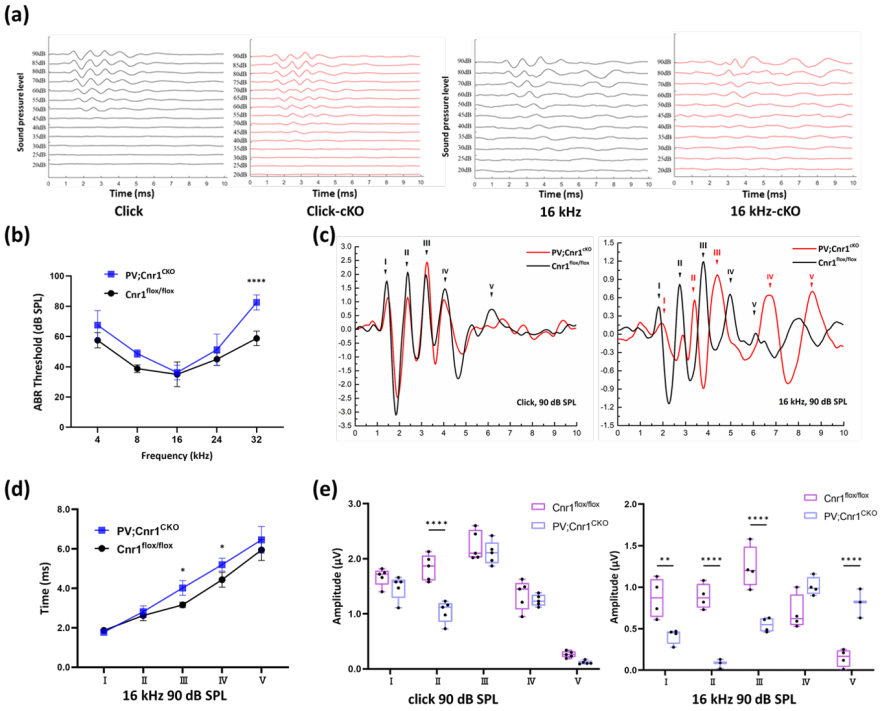

Figure. 4

Abbreviation List

Abbreviation	Full Name
2-AG	2-arachidonoyl glycerol
ABR	auditory brainstem response
AC	auditory cortex
AEA	anandamide
AVCN	**anterior ventral cochlear nucleus**
CB1R	cannabinoid receptor type 1
CBD	cannabidiol
CN	cochlear nucleus
CNIC	central nucleus inferior colliculus
CNS	central nervous system
DCIC	dorsal cortex inferior colliculus
DCN	**dorsal cochlear nucleus**
ECIC	external cortex inferior colliculus
IC	inferior colliculus
ISH	in situ hybridization
LL	lateral lemniscus
LSO	lateral superior olive
MGB	medial geniculate body
MNTB	medial nucleus of the tapezoid body
MSO	medial superior olive
PV	parvalbumin
PVCN	**posterior ventral cochlear nucleus**
SEM	**standard error mean**

Hosted file

Revised Manuscript an unmarked version.docx available at https://authorea.com/users/844774/articles/1256464-conditional-deletion-of-cb1-receptor-in-parvalbumin-expressing-gabaergic-neurons-results-in-hearing-loss-and-abnormal-auditory-brainstem-response-in-mice